Efflorescence of Ammonium Sulfate and Coated Ammonium Sulfate Particles: Evidence for Surface Nucleation

ARTICLE *in* THE JOURNAL OF PHYSICAL CHEMISTRY A · SEPTEMBER 2010

Impact Factor: 2.69 · DOI: 10.1021/jp103541w · Source: PubMed

Efflorescence of Ammonium Sulfate and Coated Ammonium Sulfate Particles: Evidence for Surface Nucleation

V. Gabriela Ciobanu,*,† Claudia Marcolli,† Ulrich K. Krieger,† Andreas Zuend,‡ and Thomas Peter†

Institute for Atmospheric and Climate Science, ETH Zürich, Zürich, Switzerland, and Department of Chemical Engineering, California Institute of Technology, Pasadena, California 91125

Received: April 20, 2010; Revised Manuscript Received: July 12, 2010

Using optical microscopy, we investigated the efflorescence of ammonium sulfate (AS) in aqueous AS and in aqueous 1:1 and 8:1 (by dry weight) poly(ethylene glycol)-400 (PEG-400)/AS particles deposited on a hydrophobically coated slide. Aqueous PEG-400/AS particles exposed to decreasing relative humidity (RH) exhibit a liquid−liquid phase separation below ∼90% RH with the PEG-400-rich phase surrounding the aqueous AS inner phase. Pure aqueous AS particles effloresced in the RH range from 36.3% to 43.7%, in agreement with literature data (31−48% RH). In contrast, aqueous 1:1 (by dry weight) PEG-400/AS particles with diameters of the AS phase from 7.2 to 19.2 μm effloresced between 26.8% and 33.9% RH and aqueous 8:1 (by dry weight) PEG-400/AS particles with diameters of the AS phase from 1.8 to 7.3 μm between 24.3% and 29.3% RH. Such low efflorescence relative humidity (ERH) values have never been reached before for AS particles of this size range. We show that these unprecedented low ERHs of AS in PEG-400/AS particles could not possibly be explained by the presence of low amounts of PEG-400 in the aqueous AS phase, by a potential inhibition of water evaporation via anomalously slow diffusion through the PEG coating, or by different time scales between various experimental techniques. High-speed photography of the efflorescence process allowed the development of the AS crystallization fronts within the particles to be monitored with millisecond time resolution. The nucleation sites were inferred from the initial crystal growth sites. Analysis of the probability distribution of initial sites of 31 and 19 efflorescence events for pure AS and 1:1 (by dry weight) PEG-400/AS particles, respectively, showed that the particle volume can be excluded as the preferred nucleation site in the case of pure AS particles. For aqueous 1:1 (by dry weight) PEG-400/AS particles preferential AS nucleation in the PEG phase and at the PEG/AS/substrate contact line can be excluded. On the basis of this probability analysis of efflorescence events together with the AS ERH values of pure aqueous AS and aqueous PEG-400/AS particles aforementioned, we suggest that in pure aqueous AS particles nucleation starts at the surface of the particles and attribute the lower ERH values observed for aqueous PEG-400/AS particles to the suppression of the surface-induced nucleation process. Our results suggest that surface-induced nucleation is likely to also occur during the efflorescence of atmospheric AS aerosol particles, possibly constituting the dominating nucleation pathway.

Introduction

Aerosol particles are ubiquitous in the troposphere and can undergo different phase transitions, such as deliquescence and efflorescence. Deliquescence refers to the dissolution of crystalline particles by uptake of water from the gas phase and can be thermodynamically predicted. In contrast, efflorescence involves nucleation of the crystalline phase in a supersaturated liquid environment, which is followed by crystal growth and rapid evaporation of water. The knowledge of the physical state of aerosol particles is important for predicting their light scattering and absorption properties[1] as well as the rate of chemical reactions that can take place either on the surface of solid particles or both on the surface and in the bulk of liquid particles.[2]

Up to now, it has not been clear how the nucleation process in supersaturated or supercooled droplets is initiated and how it proceeds. Also the location of nucleation, volume vs liquid−vapor interface, has been under debate. According to the standard notion, formation of critical nuclei takes place somewhere in the volume of a sample, and therefore, nucleation rates should scale with the sample volume. However, recently, Tabazadeh and co-workers[3,4] suggested that nucleation may take place at the surface of the droplets rather than in the volume. This conclusion was drawn after analysis of several data sets on homogeneous freezing of nitric acid dihydrate (NAD) and nitric acid trihydrate (NAT) and freezing of water droplets. It was argued that a better agreement between the data could be established when assuming surface-based rather than volume-based nucleation rates. Djikaev et al.[5] showed using the capillarity approximation that the work of formation of critical nuclei is lower at the surface than in the volume, if the condition that at least one crystal facet is only partially wettable by its own melt is satisfied.

Since then, the idea of surface nucleation has been disputed. One objection was that the experimental data the authors analyzed referred to the freezing of water droplets in emulsions.[6] The presence of the surfactant could have induced heterogeneous nucleation at the interface with the surfactant.[7] Koop[8] analyzed

* To whom correspondence should be addressed. Phone: +41-44-633-40-63. Fax: +41-44-633-10-58. E-mail: gabriela.ciobanu@env.ethz.ch.
† ETH Zürich.
‡ California Institute of Technology.

10.1021/jp103541w
Published on Web 08/16/2010

data on ice nucleation in water droplets in gaseous environments and concluded that the experimental errors associated with the published data are too large to distinguish between surface- and volume-dependent processes on the basis of measured nucleation rates. Laboratory measurements indicate that homogeneous nucleation of ice from pure water droplets is indeed a volume-proportional process for droplet radii above 19 μm.[9] These investigations could not, however, exclude the possibility that surface nucleation might be important for smaller droplets. Recently, Sigurbjörnsson and Signorell[10] showed that for submicrometer- to nanometer-sized aerosol particles the experimental uncertainties and the approximations used for data evaluation make it impossible to distinguish between surface and volume nucleation mechanisms on the basis of nucleation rates measured with current state-of-the-art instrumentation.

Indirect evidence for ice nucleation occurring at the liquid surface has been put forward by Shaw et al.[11] and Durant and Shaw.[12] They observed higher freezing temperatures and enhanced nucleation rates for droplets with an ice-forming nucleus placed close to the surface compared to at a bulk site. On the basis of these results, they suggested that contact nucleation is simply a manifestation of the enhanced surface nucleation rate. This interpretation has obtained theoretical support by computer simulations that show a tendency for nucleation at or near the surface in fluid clusters. Molecular dynamics simulations on homogeneous ice nucleation[13,14] showed that freezing starts preferentially in the subsurface layer. Zasetsky et al.[15] suggested that nucleation at the interface could be promoted by low-density domains (which the authors named "icelike clusters") caused by water density fluctuations, because of their larger size at the interface than in the bulk.

Recent studies used high-speed or normal video cameras to investigate the freezing of water droplets. Bauerecker et al.[13] observed freezing starting predominantly at the surface of acoustically levitated water droplets, whereas Hindmarsh et al.[16] observed both surface and volume ice nucleation in supercooled sucrose solution droplets suspended on the junction of a thermocouple.

In this study, using a high-speed video camera, we investigate ammonium sulfate (AS) efflorescence in aqueous AS and in aqueous poly(ethylene glycol)-400 (PEG-400)/AS particles forced by well-defined humidity cycles. Ammonium sulfate is a common salt of atmospheric aerosols, and its phase transitions as a function of relative humidity (RH) (deliquescence and efflorescence) have been intensively studied for different sizes of aerosol particles and at different temperatures.[17−27] However, there is a large scatter of data for the efflorescence relative humidity (ERH), with values ranging between 31% and 48% for particle sizes from 0.045 to 30 μm at ambient temperatures.

Field measurements have shown that atmospheric aerosols are internal mixtures of inorganic salts and organic components.[28,29] A number of laboratory studies have been performed to determine the influence of the organic components on the efflorescence of AS.[26,30−35] Organics, such as malonic, glutaric, and citric acids, glycerol, or levoglucosan, were found to decrease or even suppress the ERH of inorganic salts.[26,30,32−35] In this study, we chose PEG-400 as the organic component, a substance that induces a miscibility gap in mixtures with aqueous AS[36,37] and has no measurable effect on the deliquescence relative humidity (DRH) of AS. We investigate whether efflorescence starts at the surface or in the volume of the particles on the basis of the initial crystal growth site. We report the ERH of AS in both pure aqueous AS and aqueous PEG-400/AS particles deposited on a hydrophobically coated substrate and provide a comparison of our data with existing literature values on AS ERH.

Experimental Section

The setup used in our experiments is described in detail elsewhere.[37] An Olympus microscope (BX-40) combined with a high-speed PCO video camera (set to 1420 frames/s) was used to monitor AS efflorescence in aqueous AS and aqueous PEG-400/AS particles. An additional standard CCIR video camera (25 frames/s) was used to record the ERH and the further evolution of the AS efflorescence. During the experiments, images were stored temporarily in the ring buffer of the PCO camera. When an event occurred (i.e., changes in the particle brightness between two subsequent frames taken with the CCIR video camera (time difference 40 ms)), a custom-made program, implemented in Matlab, was used to initiate the permanent saving of the frames (~60 000 frames) stored in the ring buffer just before and after the trigger signal.

AS (Fluka, 99.5%) and PEG-400 (Fluka, 91893, BioUltra) were used without further purification to produce AS and aqueous PEG-400/AS particles. Small crystals of AS were obtained by cutting larger crystals, whereas the aqueous PEG-400/AS particles were produced with a droplet generator (a modified Hewlett-Packard inkjet cartridge, model HP 51604A) from aqueous solutions (prepared by weight with Milli-Q water, resistivity 18.2 MΩ, using an analytical balance). The particles were deposited on a previously silanized (hydrophobically coated) microscope slide mounted on the sample holder of a heating/cooling cell (Linkam, model LTS 120). The RH inside the cell was adjusted by mixing dry N_2 and water-saturated N_2 flows using automatic mass flow controllers. The RH was measured with a G-TUCN.34 (UPSI, France) humidity sensor with an accuracy of $\pm$2% in the range of 2−98%. During the experiments the temperature inside the cell and in the gas phase was maintained at 293 $\pm$ 0.1 K, while the RH was decreased at a rate of $d(RH)/dt = -0.3\%/min$. In the first step the particles were exposed to high RH to deliquesce the ammonium sulfate, and subsequently, the RH was decreased below the AS ERH. The size of the investigated particles (the dry diameter) ranged from 16 to 31 μm for AS particles, from 16 to 35 μm for 1:1 (by dry weight) PEG-400/AS particles, and from 44.8 to 46.9 μm for 8:1 (by dry weight) PEG-400/AS particles. The sizes specified for the particles in the present study refer to the diameter of the base area of the particle in contact with the substrate viewed in the microscope. The morphological changes during AS efflorescence were recorded with the high-speed video camera, and the images obtained were used to study the efflorescence process.

Results and Discussion

Influence of the Organic (PEG) Coating on the AS ERH. Aqueous PEG-400/AS particles show a liquid−liquid phase separation below RH $\approx$ 90% into an aqueous AS phase surrounded by a (aqueous) PEG phase. Different phases can be well discriminated by optical microscopy, and their composition is subsequently established by micro-Raman spectroscopy. Figure 1 shows the ERH of AS as a function of the particle size for pure aqueous AS particles and aqueous 1:1 and 8:1 (by dry weight) PEG-400/AS particles investigated in this study (solid symbols). Also shown are literature data of pure aqueous AS particles investigated by different techniques as listed in Table 1 (electrodynamic balance (EDB), optical microscopy on deposited particles, aging chamber (AC), hygroscopicity tandem differential mobility analyzer (HTDMA), and flow tube system

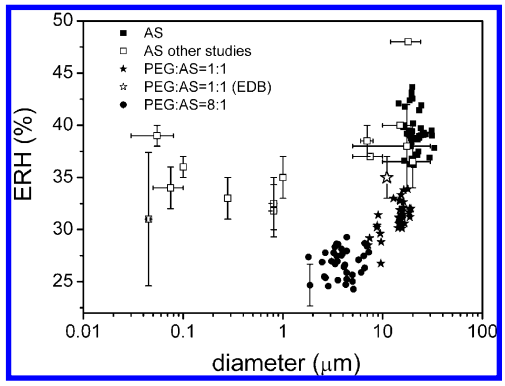

Figure 1. AS ERH as a function of the diameter of the AS phase from literature data (open squares; error bars give the range of measured particle diameters and ERH) and the present work (filled symbols). The AS ERH values from the literature are listed in Table 1, together with the corresponding references. "EDB" refers to single levitated droplets investigated in an electrodynamic balance. The uncertainty of our experimental data is indicated as an error bar for one data point.

TABLE 1: Experimental Studies of AS Efflorescence from the Literature

ref	diam (μm)	ERH (%)	technique[a]	temp (K)
18	12.0−24.2	48	EDB	293
25	5−30	34.3−42.5	microscopy	293.2
35	10−20	40	EDB	291
17	0.03−0.08	38−40	AC	298
19	6−8	37−40	EDB	298
26	10−30	34−39	microscopy	295−300
20	5−10	37	EDB	298
27	0.1	35−37	HTDMA	293
21	1	35 ± 2	FTS/FTIR	298
23	0.05−0.1	34 ± 2	HTDMA	298
[b]	0.28	33 ± 2	FTS/FTIR	298
22	0.75−0.87	32.5 ± 2.5	FTS/FTIR	295
22	0.75−0.87	31.8 ± 2.5	FTS/FTIR	293.5
24	0.043−0.047	31 ± 6.4	HTDMA	298

[a] EDB = electrodynamic balance, AC = aging chamber, HTDMA = hygroscopicity tandem differential mobility analyzer, and FTS = flow tube system. [b] Cziczo, D. J.; Nowak, J. B.; Hu, J. H.; Abbatt, J. P. D. Infrared Spectroscopy of Model Tropospheric Aerosols as a Function of Relative Humidity - Observation of Deliquescence and Crystallization. *J. Geophys. Res.* **1997**, *102* (D15), 18843−18850.

with FTIR detection (FTS/FTIR)). Note that the ERH values for aqueous PEG-400/AS particles are given as a function of the dry diameter of the AS phase inclusions to establish comparability of the pure AS and PEG-400/AS particles.

Literature values for efflorescence of pure aqueous AS particles are distributed over a large range of RH: the lowest values (31 ± 6.4%) were measured by Gao et al.[24] for 43−47 nm particles and the highest (up to 48%) by Cohen et al.[18] for 12−24 μm particles in an EDB. Typical values obtained by several groups are in the range of 35−40% RH. Values above 40% are suspected to occur due to heterogeneous impurities.[1] General inspection of all literature data suggests a slight increase of AS ERH with increasing particle diameter. Such an increase has also been postulated by Gao et al.,[24] who evaluated their own measurements together with literature data for AS particles spanning the size range from 8 nm to 17 μm utilizing the framework of classical nucleation theory. Most ERH values measured for pure aqueous AS particles in this study are between 36% and 40%, i.e., within the typical range for AS nucleation of micrometer-sized particles, with some efflorescence events occurring between 40% and 44%. We did not observe any size dependence of AS efflorescence in our data set.

In contrast to pure AS, in aqueous PEG-400/AS particles AS effloresced between 24.3% and 33.9% RH (namely, 26.8−33.9% RH in aqueous 1:1 and 24.3−29.3% RH in aqueous 8:1 (by dry weight) PEG-400/AS particles). This is significantly lower than all reported values for pure aqueous AS particles of the same size range. Moreover, for these particles we find a significant size dependence, with a linear correlation coefficient $R = 0.86$: an increase of 1 μm in the diameter of the particle corresponds to an increase of 0.4% in ERH. This diameter dependency of ERH (0.4%/μm) is in the range of the diameter dependency of ERH for pure AS particles (0.06−1.2%/μm for particles with diameters in the range from 0.05 to 30 μm), as evaluated by Gao et al.[24] Marcolli and Krieger[36] measured slightly higher AS ERH values (33−37%) for an aqueous 1:1 (by dry weight) PEG-400/AS particle in the EDB with a dry diameter of ∼11 μm for the AS phase (open star in Figure 1).

In the following we intend to disprove a number of arguments that our observations were caused by (1) the interactions between the organic and inorganic components within the predominantly inorganic phase, (2) a kinetic effect of the organic coating impeding H_2O evaporation, or (3) instrumental or experimental artifacts.

(1) Interactions between the Organic and Inorganic Components. Different studies have shown that in the presence of organic components the ERH of AS may be decreased or even suppressed when the fraction of organics is large.[26,30,32−35] In contrast to these studies, where the organic component was fully miscible with the inorganic salt, PEG-400 forms a separate phase in the particles at RH below ∼90%. Due to this phase separation there is no significant amount of organic matter in the aqueous AS phase: analysis by Raman spectroscopy[37] showed that the amount of PEG-400 is below 1.6 wt % of the dry mass at 78% RH. On the basis of the experimentally determined phase diagram,[37] PEG-400 contributes less than 3 wt % of dry mass to the AS phase below 80% RH. The phase diagram calculated with the aerosol inorganic−organic mixtures functional groups activity coefficients (AIOMFAC) model[38−40] extended by the oxyethylene group (−CH_2OCH_2−) of PEG indicates less than ∼1 wt % PEG-400 at 80% RH and virtually no PEG-400 at 40% RH in the aqueous AS phase ($<10^{-11}$ wt %, corresponding to no PEG molecules at all in the aqueous AS-rich phase for typical diameters of the AS-phase inclusions (2−20 μm diameters)). Therefore, the decrease of the AS ERH cannot be explained as a result of molecular interactions between the organic substance and the inorganic salt. Because the presence of PEG increases the mean activity coefficient (and the ion activity product) of AS, the ERH of AS is expected to shift to higher rather than to lower RH when AS and PEG-400 are present in the same phase. Evaluation of the AS ion activity product with AIOMFAC indicates that the supersaturation of AS as a function of the RH in PEG-400/AS mixtures shows approximately the same trend as in pure AS solutions due to the virtually complete phase separation. For AS efflorescence occurring at ∼32% RH the AS ion activity product is ∼50% higher than for AS efflorescence at 40% RH. Therefore, we conclude that AS efflorescence in PEG-400/AS particles occurs at higher supersaturations (higher ion activity products) than in pure AS particles. Furthermore, because the main interaction between PEG and AS is repulsive, the interference of PEG molecules with the surface integration of AS into the growing crystal embryo is unlikely. Also, the size of the PEG molecule in comparison to AS units is very different, which makes it unlikely that PEG-400 would block incorporation of AS units into kink sites of the growing crystal, a mechanism that has

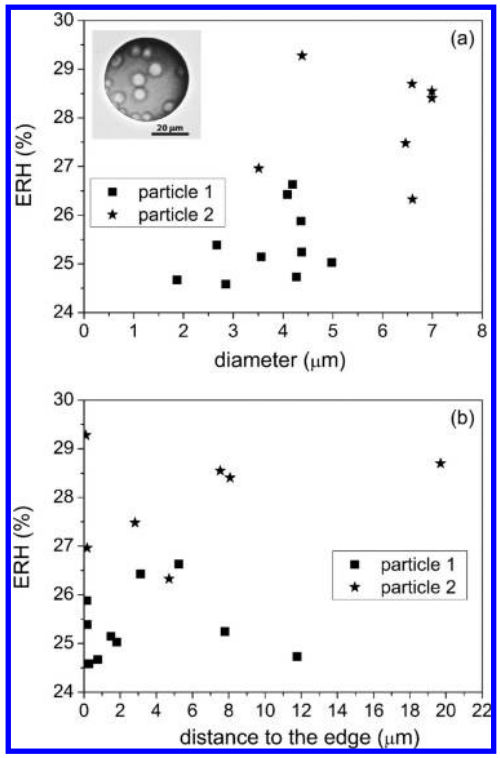

Figure 2. ERH of aqueous AS inclusions in two selected 8:1 (by dry weight) PEG-400/AS particles as a function of the inclusion dry diameter (a) and distance to the edge (b). See the inset for a typical distribution of aqueous AS inclusions in one of the particles.

previously been suggested as an effective suppressor of nucleation of organic molecules with similar sizes.[41]

(2) Impedance of H_2O Evaporation by the Organic Coating. Organic coatings can inhibit the evaporation of water and consequently be a reason for an apparent shift in the ERH of inorganic salts to lower values[42] when the RH is decreased at a high rate. To determine whether the PEG coating could have exerted a kinetic effect on water evaporation, we estimated the diffusion time necessary for water molecules to diffuse from the inner aqueous AS phase through the PEG coating using the following relation:[43]

$$\tau = \frac{x^2}{6D_w} \quad (1)$$

where x is the thickness of the PEG coating and D_w the diffusion coefficient of water in the PEG phase. We chose for our calculations $x = 4.5$ μm (i.e., the thickness of the outer phase of the PEG-400/AS particle shown in Figure 8a). With a diffusion coefficient $D_w = 2.5 \times 10^{-7}$ cm^2/s at 298 $\pm$ 0.01 K[44] for water in an aqueous PEG-400 solution with 88.43 wt % PEG-400 (i.e., the concentration observed for PEG-400 at ~50% RH[36]), we obtain $\tau = 0.14$ s, which is fast considering the rate of change of RH used for the experiments (d(RH)/dt = 0.005%/s). Consequently, the low AS ERH values in PEG-400/AS particles are not due to hindered water diffusion caused by the organic coating.

Analysis of AS efflorescence in aqueous 8:1 (by dry weight) PEG-400/AS particles also supports the conclusion drawn above. In contrast to the 1:1 (by dry weight) PEG-400/AS particles, for the 8:1 composition the AS inner phase is distributed as small inclusions in the PEG phase (see the inset in Figure 2a). Figure 2 gives the ERH observed for each AS inclusion as a function of the dry diameter (panel a) and as a function of the minimum distance to the edge of the particle's 2D projection (panel b) of two selected particles. As can be seen in Figure 2b there is no clear tendency for inclusions that are closer to the edge to effloresce first. An AS inclusion found at 20 μm from the edge effloresced earlier than one at just 0.1 μm from the edge. However, we observe a tendency of larger inclusions to effloresce at higher RH (Figure 2a). From the efflorescence behavior of AS inclusions we can conclude that indeed the PEG-400 coating does not impede water evaporation significantly.

(3) Instrumental or Experimental Artifacts. Homogeneous nucleation is a stochastic process with a nucleation rate that is a function of supersaturation (and to a lesser degree of temperature). Therefore, there should be an increase of ERH with increasing observation time. When we compare the time scales of the different experimental techniques used to measure the AS ERH, the observation times of our setup (optical microscopy of deposited particles) and EDB are in the range of minutes while the observation times for FTS/FTIR and HTDMA are on time scales of seconds. Therefore, differences in the observation time cannot explain the low ERH that we observed for coated AS particles.

One major difference between pure aqueous AS and aqueous PEG-400/AS particles is that the air/droplet interface of the pure AS particles is replaced by the PEG/aqueous AS interface in particles with a PEG coating. We speculate therefore that the lower AS ERH values of the coated particles may be explained by differences in the nucleation process: if AS efflorescence in pure aqueous AS particles was initiated by nucleation at the air/droplet interface, this surface-induced nucleation would no longer be viable in the presence of the PEG coating. Nucleation should therefore rather start in the volume of the aqueous AS phase in the case of aqueous PEG-400/AS particles.

High-Speed Photography of the Efflorescence Process. Some of the experiments presented in Figure 1 have been recorded with a high-speed video camera. High-speed photography allows resolving very fast processes occurring on the time scale of milliseconds such as efflorescence and freezing. In this paper, we deduce the site of AS nucleation in aqueous AS and aqueous PEG-400/AS particles deposited on a hydrophobically coated glass slide on the basis of the initial crystal growth site and follow the progression of crystallization fronts using the high-speed video camera. Further crystal growth accompanied by water loss is recorded with the second video camera.

Efflorescence of Pure Aqueous AS Particles. Crystallization of AS during efflorescence takes place in several stages.[45,46] In the first stage, critical nuclei, having a composition similar to that of the bulk solid, form in a supersaturated solution. This nucleation stage is often described in an approximate manner by means of classical nucleation theory, which results in an Arrhenius-like expression for the nucleation rate. In the second stage, a supercritical nucleus grows until the supersaturation in the solution is consumed. This first growth stage takes place without significant water loss of the particle to the gas phase and is therefore accompanied by a rapid increase of water activity in the remaining liquid. To balance the lower water vapor pressure of the surrounding gas phase, water evaporation from the particle sets in, leading to the third stage of AS efflorescence, which is characterized by concomitant crystal growth and water evaporation. While crystal growth during the second stage is limited by liquid-phase diffusion of ammonium and sulfate ions in the aqueous solution, the progress of the third stage depends on water diffusion through the crystalline AS phase that has formed on the surface of the particle.

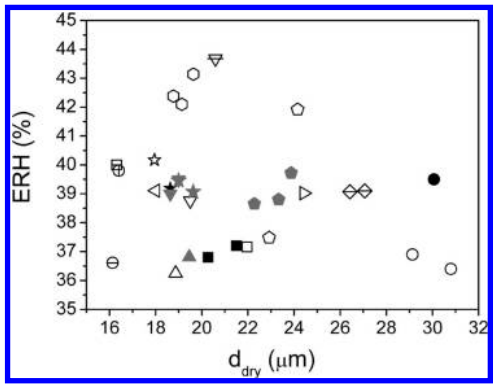

Figure 3. ERH of AS as a function of the dry diameter for pure aqueous AS particles that have been monitored by the high-speed video camera. Different symbols refer to different particles. The symbol color indicates the site of initial crystal growth: white, rim region; black, inner region; gray, unclear.

We monitored AS efflorescence for 14 pure aqueous AS particles using the high-speed video camera. Some of the particles were exposed to several humidity cycles to investigate the possibility of having heterogeneous nuclei triggering the efflorescence, leading to a total of 31 efflorescence events. Figure 3 summarizes all these measurements and gives the ERH of AS as a function of the particle dry diameter. In this graph, different symbols refer to different particles. Particles were cycled one (e.g., left- and right-pointed triangles) to five times (pentagons). In general, a slight increase in the particle diameter (maximum 2 μm) with increasing number of humidity cycles was observed, which we ascribe to a decrease of the contact angle while the particle shrinks and grows during humidity cycles. The AS ERH ranges from 36.3% to 43.7% for particle sizes from 16 to 31 μm in dry diameter.

Figure 4 shows two examples of efflorescence starting (a) from the inner region and (b) from the rim region of the particle's 2D projection. The growth of the initial crystals and the morphological changes of the particle are shown by a series of frames taken at different times. Time was set to zero for the frame before the initial crystal growth was observed. Figure 4a exemplifies the efflorescence of a particle for which initial crystal formation appears in the inner region of the particle's 2D projection at RH = 39.5%. The initial crystal has an X-shape which elongates in all four directions after 1.4 ms (third frame of Figure 4a). Crystal growth proceeds until half of the particle is covered at t = 2.1 ms after initial detection of the phase change. The crystallization front propagates to the other half of the particle until at t = 4.9 ms the particle is fully covered with a crystalline coating. We interpret this fast growth of a crystalline layer as the first crystal growth stage that is accompanied by hardly any water loss. Further morphological changes were observed as darker regions moving through the particle. It has been reported previously that water was found in effloresced particles;[47,48] therefore, these regions could correspond to water pockets trapped inside the AS crystal. A movie showing the efflorescence of this AS particle recorded with the high-speed camera is available (see the Supporting Information). The last image of Figure 4a shows the morphology of the deeply dehydrated particle (no morphological changes were observed after this time when the RH was further decreased), recorded with the second video camera at RH = 38.4%. It marks the end of the second crystal growth stage with concomitant crystallization and evaporation.

In Figure 4b the growth of crystalline AS started in the rim region of the particle's 2D projection at 43.7% RH. First, a main branch is observed, followed by the growth of additional branches on both sides of the main branch, resulting in a dendritic-like pattern that covers the whole surface of the particle at t = 6.3 ms and marks the end of the first crystal growth stage. Similar to the previous case, further changes occurred much more slowly and can be seen by comparing the frame at 6.3 ms to that at 2.6 s. A movie showing the efflorescence of this AS particle recorded with the high-speed video camera is available (see the Supporting Information). Again, the last frame of Figure 4b shows the deeply dehydrated particle after ~2 min at 43.1% RH.

To illustrate clearer the initial crystal growth site for the particles shown in Figure 4, the second and the third frames have been divided by the first frame for each series using the ImageJ software.[49,50] The edge of the particles was added after the division. The results in Figure 5 show that for the particle

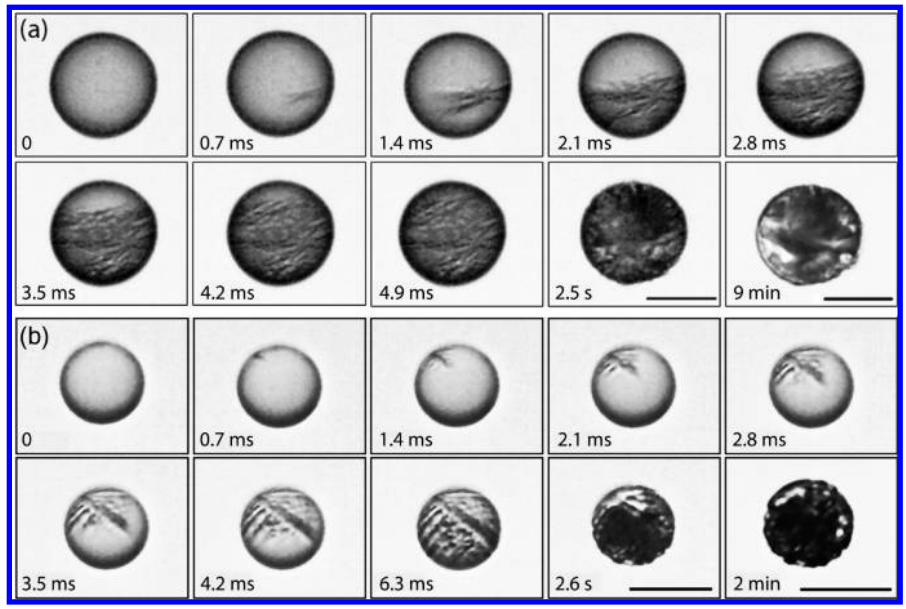

Figure 4. Examples of AS crystal growth in pure aqueous AS particles starting from (a) the inner region and (b) the rim region of the particle's 2D projection. The bars in the last two frames represent 20 μm.

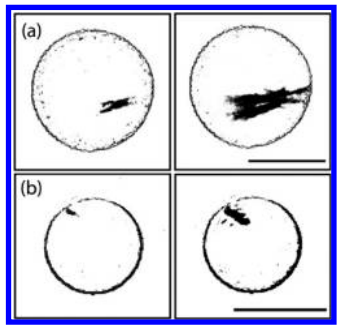

Figure 5. Ratios between the second and first frames and the third and first frames of each series of Figure 4. Panel a shows the initial crystal growth site in the inner region of the particle. Panel b shows the initial crystal growth site in the rim region of the particle. The bars in the frames represent 20 μm.

in Figure 4a the initial crystal site is in the inner of the particle's 2D projection whereas for the particle shown in Figure 4b the crystal growth starts in the rim region of the particle's 2D projection.

The image sequences shown in Figure 4 indicate that during the first crystal growth stage a shell forms on the surface of the particles. Shell formation has been previously reported for sea salt and aqueous NaCl particles.[51,52] The thickness of this shell can increase as long as the solution trapped inside the particle is supersaturated. We have estimated the thickness of such a solid shell for a 20 μm radius particle to be ~20% of the initial radius of the particle. The calculation was made on the basis of the concentration of a supersaturated AS solution before efflorescence (77.4 wt % AS aqueous solution at 39.5% RH) and with the assumption that water does not evaporate from the droplet during growth of the solid shell and therefore growth of the crystal stops when a saturated solution remains (43 wt % AS aqueous solution at 80% RH). The concentration of the supersaturated AS solution at 39.5% RH was determined using the AIOMFAC model.[38−40]

We used the optical 2D images of the particles for a systematic evaluation of the efflorescence of AS with special attention given to the nucleation site (taken as the site where the crystal growth was detected first). For the image analysis we sectioned the top view of the particles into a 2 μm rim region and an inner region. Given this criterion, the initial crystallization could be located either in the rim region or in the inner region of the particle's 2D projection. The 2 μm criterion was chosen on the basis of the resolution of the images to ensure a clear discrimination between the rim and inner regions. Figure 6 shows the percentage of nucleation occurrence in the rim and inner regions of the particle's 2D projections. For 61.3% of the analyzed images the first crystal appeared in the rim region and for 12.9% in the inner region. For 25.8% of the analyzed images the initial crystal could not be assigned to either the inner or rim region with the available optical contrast and time resolution, which contributes to the uncertainty of this analysis procedure. Nucleation events of particles that have been exposed to only one drying cycle are indicated by white bars in Figure 6, while nucleation events of particles for which several drying cycles were performed are marked by different colors. Comparison of color bars on the left side of Figure 6 shows that, for the particular particles represented by green, blue, and brown colors, AS nucleation occurred during some cycles in the rim region and during other cycles in the inner region of the particles' 2D projections. This shows that nucleation does not occur always at the same site in a particle (e.g., at an unrecognized heterogeneous inclusion). This is also shown in Figure 3, where nucleation events occurring in the inner region are displayed as solid black symbols and the ones occurring in the rim region are displayed as open symbols. Inspecting the ensemble of all nucleation events, crystallization in the inner region started on average at slightly lower RH than in the rim region. However, when focusing on individual particles, no such trend can be observed: e.g., the particle represented by circles in Figure 3 nucleated at 39.5% RH in the inner region (black circle) and at 36.4% and 36.9% RH in the rim region (open circle). The synopsis of evidence shows the stochastic nature of the nucleation process.

For a droplet deposited on a substrate there are several possible sites where crystal nucleation can occur: (1) at the air/droplet interface, (2) in the volume of the droplet, (3) at the droplet/substrate interface, and (4) along the air/droplet/substrate contact line (see the schematic representations in Figure 6 for an illustration). To determine whether AS nucleation showed a preference for one of these four sites, we evaluated the probability of observing nucleation either in the 2 μm rim region or in the inner region of the 2D projection of a particle viewed from the top for these four nucleation scenarios. The volume and the surface area of the rim region and inner region of the

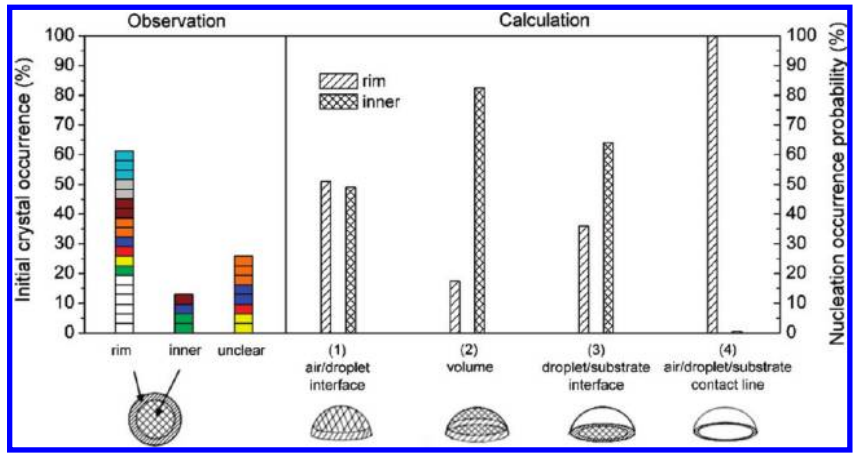

Figure 6. Apparent site of nucleation occurrence observed in the aqueous AS particle's 2D projection (left part) compared with the calculated probability of the nucleation site (right part) at the air/droplet interface (1), in the volume (2), at the droplet/substrate interface (3), and at the air/droplet/substrate contact line (4). Site attribution "rim" assumes a crystal to be observed in or calculated for a rim region of 2 μm for the particles 2D projection. Calculations assume a particle with a 10 μm radius and a contact angle of 83° with the substrate (as measured for a saturated aqueous AS droplet).

particles were calculated assuming a contact angle of the droplet with the substrate of 83°, as measured for larger saturated AS particles,[37] and using the 2 μm thickness of the rim region criterion. The calculation part on the right-hand side of Figure 6 shows the expected distribution for the four nucleation sites. When the results obtained from image analysis (observation) are compared with the probability calculations, the best qualitative resemblance is reached for nucleation and growth from the air/droplet/substrate contact line or for nucleation at the air/droplet interface. The particle volume and the droplet/substrate interface can be excluded as preferential sites for AS nucleation because, in contrast to the observations, the inner region of the droplet should have been observed as the preferred nucleation site.

The contact line has indeed been shown both theoretically and experimentally to be a favored site for nucleation. Inspired by the contact freezing mode of ice, Sear[53] modeled that nucleation rates at the contact line are higher than at any other interfaces. They explain this finding by classical nucleation theory. At a contact line three interfaces meet. As the nucleus expands, the areas of all these interfaces are reduced and the corresponding reduction in the interfacial free energy directly contributes to a reduction in the height of the free energy barrier to nucleation. Contact lines have also been proposed to be preferred nucleation sites for nanowire growth. This is explained by the supersaturation of the solution that is highest at the contact line.[54] For water droplets on silicon surfaces treated with various silanes, freezing was observed to preferably occur from the three-phase contact line of the solid−water contact area.[55] Crystallization at the contact line has also been observed for salt particles deposited on substrates (e.g., Na_2SO_4[56] and $NaClO_4$[57] droplets). This phenomenon was explained by the fact that evaporation at the rim of the droplet is more effective because the probability of evaporated solvent recondensing on the droplet is less than near the top of the droplet.[58] Consequently, the supersaturation is higher at the rim of the particle, leading to a higher nucleation probability in that zone as compared to the top of the droplet.

On the basis of the present analysis it is not possible to locate the nucleation site in the particle with any certainty, also because combinations of the nucleation sites might be possible. However, it is likely that the traditional assumption of a dominant volume-based nucleation mode is incorrect. It is likely that the contact line plays an important role, but it is clear that it alone cannot explain the observations. We therefore conclude that the contact line probably together with the particle surface is the preferred site for AS nucleation.

Efflorescence of AS in Aqueous PEG-400/AS Particles. Ten aqueous 1:1 (by dry weight) PEG-400/AS particles have been monitored using the high-speed video camera, and a total of 19 efflorescence events have been observed. Figure 7 summarizes these measurements and gives the ERH of AS as a function of the particle dry diameter as well as the number of exposures to drying cycles (same symbol). The ERH ranges from 28.8% to 33.8% for particle sizes between 16 and 35 μm (total dry diameter). A slight dependence of the ERH on the particle size is observed in this case. In contrast to the pure aqueous AS particles, there was no significant change in the apparent diameter of the particles with increasing number of humidity cycles. This may be a result of the interaction of the PEG phase with the hydrophobic substrate, which might lead to a constant contact angle.

Figure 8 shows two examples of efflorescence starting (a) inside the AS phase and (b) from the PEG-400/AS interface of

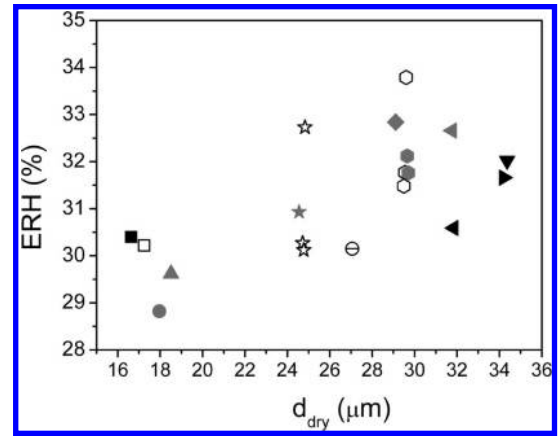

Figure 7. AS ERH of aqueous 1:1 (by dry weight) PEG-400/AS particles that have been monitored by the high-speed video camera. Different symbols refer to different particles. The symbol color indicates the site of initial crystal growth: white, AS-phase region; black, PEG/AS interface region; gray, unclear.

the particle. In Figure 8a nucleation occurs in the aqueous AS phase, at RH = 30.1%, and crystal growth proceeds until the AS phase is covered after 2.8 ms. Further changes occur much more slowly in the particle (t = 2800 ms). A movie showing the efflorescence of the AS inner phase recorded with the high-speed video camera is available (see the Supporting Information). In Figure 8b the crystal starts to grow from the PEG-400/AS interface. The crystallization front propagates until it covers the whole AS phase at t = 4.9 ms and RH = 30.6%. In contrast to the case shown in Figure 8a, no significant changes in the arrangement of the PEG and AS phases are observed for this particle after ~2500 ms, illustrating the variations in crystal growth that seem to exist for such particles. A movie showing the efflorescence of the AS inner phase recorded with the high-speed video camera is available (see the Supporting Information).

ImageJ software[48,49] has been used to obtain a clearer illustration of the initial crystal growth sites, by dividing the second and the third frames by the first frame for each series of Figure 8. The edge of the particles and the 2 μm PEG-400/AS interface were added after the division. The results are shown in Figure 9. The image processing reveals more clearly that for the particle shown in Figure 8a the initial crystal site is in the AS phase whereas for the particle shown in Figure 8b the crystal growth starts at the PEG-400/AS interface.

In PEG-400/AS particles, efflorescence can in principle have its origin in the aqueous PEG-rich phase or in the aqueous AS-rich phase. Assuming all components are in thermodynamic equilibrium, the AS supersaturation is in both phases the same; however, the concentration of AS is much lower in the PEG-rich phase, making a nucleation much less likely. In the 2D projection of the particles, the PEG phase appears as an outer ring that surrounds the aqueous AS phase. In a previous paper,[37] we derived the 3D morphology of the PEG-400/AS particles for different dry mass ratios of PEG-400/AS on the basis of the observed 2D projections and the volume ratios of the organic to inorganic aqueous phases that we determined in bulk measurements. For a 1:1 (by dry weight) PEG-400/AS particle the two liquid phases form most likely spherical calottes of the same height with contact angles of 52° and 73 ± 2° for the outer and inner calottes, respectively. We assume that the air/particle interface is totally wetted by the PEG phase because of the surface-active properties of poly(ethylene glycol) and its ability to form monolayers at the air/water interface.[59] To

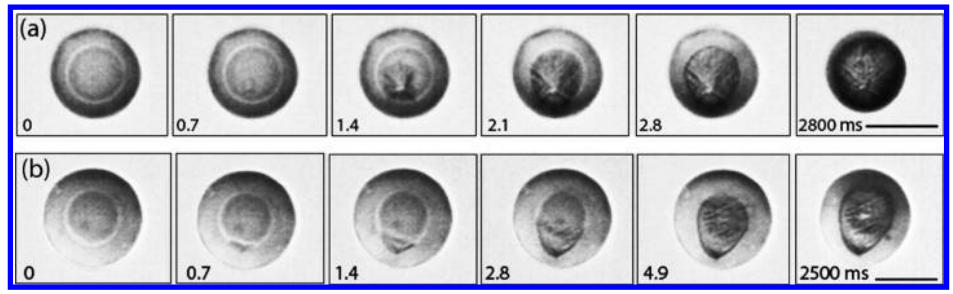

Figure 8. Examples of AS crystal growth in aqueous 1:1 (by dry weight) PEG-400/AS particles starting (a) from the AS phase and (b) at the PEG-400/AS interface. The bars in the rightmost frames represent 20 μm.

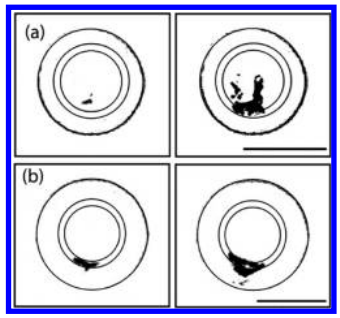

Figure 9. Ratios between the second and first frames and the third and first frames of each series of Figure 8. Panel a shows the initial crystal growth site in the AS phase. Panel b shows the initial crystal growth site at the PEG/AS interface. The PEG-400/AS interface region is represented by two concentric circles with a radius difference of 2 μm. The bars in the frames represent 20 μm.

evaluate the nucleation occurrence depending on the site, we divided the 2D projection of each particle into three parts: the outer PEG-rich section, the PEG-400/AS interface, and the inner AS-rich section. We attributed a thickness of 2 μm to the PEG-400/AS interface (which is about the thickness of the bright ring observed between AS and PEG phases, given the resolution and optical limitations of our microscope setup). The analysis of the 19 observed nucleation events is shown in Figure 10. Again, for the analysis we considered particles that have been exposed to one or several humidity cycles to investigate the possibility of having heterogeneous nuclei triggering the efflorescence. There was no case where we could observe initial crystal growth in the outer PEG-rich section. Initial crystals were observed more often in the AS-rich section (42% of the investigated cases) than at the PEG-400/AS interface (21%). For the rest of the cases, the nucleation site could not be identified. If we assumed that crystallization occurred with equal probability in both phases, we should have observed at least some nucleation events in the PEG-rich section. This is illustrated in the center panel of Figure 10 (PEG phase included). For these calculations, we discriminated three cases: (1) nucleation at the air/droplet interface, (2) nucleation in the volume, and (3) nucleation at the droplet/substrate interface. Assuming equal nucleation probability independent of the particle phase, nucleation should have been most often observed in the outer ring of the PEG-rich phase for nucleation at the air/droplet and the droplet/substrate interfaces. For volume nucleation, approximately every fourth nucleation event should have occurred in the PEG-rich section. Therefore, we exclude the PEG phase as the possible site for AS nucleation. Nucleation in this phase is indeed improbable because of its negligible AS concentration. In the further analysis (right panel of Figure 10, PEG phase excluded) we therefore only considered (1) the PEG-400/AS interface, (2) the volume, (3) the AS/substrate interface, and (4) the PEG/AS/substrate contact line (see the schematic representations in Figure 10 for an illustration) as possible sites for AS nucleation. The comparison of the experimental results

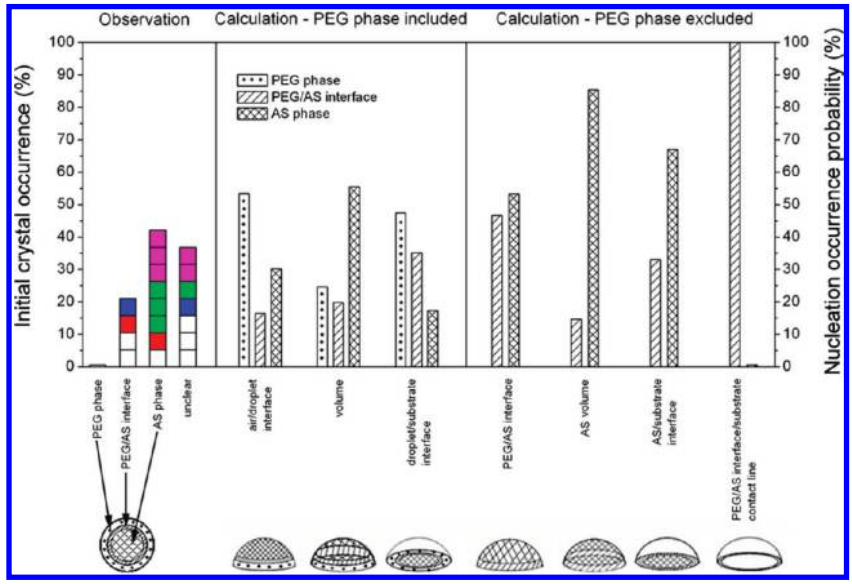

Figure 10. Apparent site of nucleation occurrence observed in the 2D projections of aqueous PEG-400/AS particles (left panel) compared with the calculated probability of nucleation for two nucleation scenarios: calculation for equal probabilities of nucleation in the PEG-rich and AS-rich phases assuming a PEG-400/AS interface of 2 μm thickness and a contact angle of 73° (center panel); calculation assuming zero probability of nucleation in the PEG-rich phase and a radius of 10 μm for the AS-rich phase (right panel).

with the calculated nucleation probabilities for these four sites indicates that the PEG/AS/substrate contact line is not a preferred nucleation site. However, on the basis of the observed distribution, we cannot exclude any of the other three nucleation sites.

Summary and Conclusions

We have measured the ERH of AS in aqueous AS and PEG-400/AS particles deposited on a hydrophobically coated substrate. The ERH of pure aqueous AS particles was between 36.3 and 43.7%, which is in the same range as the values reported in the literature for similar sizes of the particles. The ERH in pure aqueous AS did not show any significant dependence on particle size, which is in agreement with previous experiments.[25,26] In aqueous PEG-400/AS particles, however, the AS ERH was reduced to unprecedented low values between 24.3% and 33.9% RH and showed a significant dependence on the size of the particles. The presence of low amounts of PEG-400 in the inner AS phase, impedance of water evaporation through the PEG coating, or different time scales between experimental techniques cannot explain the low ERH of AS in aqueous PEG-400/AS particles.

Analysis of the distribution of initial AS crystal growth sites observed with a high-speed video camera suggests that the droplet volume is not the preferred nucleation site for efflorescence occurring in the RH range from 36.3% to 43.7%. Rather, nucleation sites occur preferentially in the vicinity of the liquid/vapor interface. Only at lower RH, in the range from 28.8% to 33.8%, are the observations with the high-speed video camera in accordance with a nucleation process originating in the volume of the AS phase, whereas nucleation starting at the interface of the AS phase (to the substrate or to the PEG phase) also cannot be excluded.

In micrometer-sized aqueous AS particles, efflorescence occurs over quite a broad RH range. Within this range different nucleation sites seem to be in competition, preventing a clear assignment of the nucleation site to either the surface or volume. Nevertheless, on the basis of this study and literature data, the following conclusions can be drawn: (1) For ERH > 40% nucleation is favored at the aqueous AS/substrate contact line (because such high values are rarely found for AS particles suspended in air). (2) In the range from 36% to 40% RH, the surface of the particle or the contact line seems to be the dominant nucleation site. (3) Volume-based nucleation only seems to become important below 34%, when nucleation at the surface and at the contact line of the particle is suppressed by the PEG-400 organic coating.

On the basis of thermodynamic arguments and analysis of experimental nucleation rates, Tabazadeh and co-workers[3−5] suggested that homogeneous nucleation would start preferentially at the surface rather than in the bulk. Their work initiated the discussion and reanalysis of the available data for homogeneous ice nucleation as well as new theoretical and experimental studies on ice freezing,[9,11,12,14] however with no conclusive answer in favor of or against surface nucleation for small particles (<1 μm).[10] Our experiments with efflorescing particles consisting of AS and PEG-400/AS together with the evaluation of literature data suggests that surface nucleation may indeed occur in the atmospheric particles, during AS efflorescence, and might constitute an important, possibly even dominating, nucleation pathway.

Acknowledgment. This work was supported by the Swiss National Science Foundation under Contract No. 200020-103651/1 supporting the Ph.D. work of V.G.C. and under Contract No. PA00P2_126227 for an Advanced Researchers Fellowship of A.Z. This work was also supported by the Competence Center Environment and Sustainability of the ETH Domain (CCES) with Project IMBALANCE supporting A.Z. before receiving his fellowship. We thank Thomas Koop for useful comments.

Supporting Information Available: Four movies showing the efflorescence of AS in pure aqueous AS and aqueous 1:1 (by dry weight) PEG-400/AS particles. Each of the first frames of the movies is inserted 15 times to show the first crystal growth stage in slow motion. Afterward, the movies are sped up. Movie 1 shows the efflorescence of AS in a pure aqueous AS particle (shown in Figure 4a) for which the initial crystal growth site was observed in the inner region of the particle's 2D projection. Movie 2 shows the efflorescence of AS in a pure aqueous AS particle (shown in Figure 4b) for which the initial crystal growth site was observed in the rim region of the particle's 2D projection. Movie 3 shows the efflorescence of AS in an aqueous PEG-400/AS particle (shown in Figure 8a) for which the initial crystal growth site was observed in the AS phase. Movie 4 shows the efflorescence of AS in an aqueous PEG-400/AS particle (shown in Figure 8b) for which the initial crystal growth site was observed at the PEG-400/AS interface. This material is available free of charge via the Internet at http://pubs.acs.org.

References and Notes

(1) Martin, S. T. Phase Transitions of Aqueous Atmospheric Particles. *Chem. Rev.* **2000**, *100* (9), 3403–3453.

(2) Ravishankara, A. R. Heterogeneous and Multiphase Chemistry in the Troposphere. *Science* **1997**, *276* (5315), 1058–1065.

(3) Tabazadeh, A.; Djikaev, Y. S.; Hamill, P.; Reiss, H. Laboratory Evidence for Surface Nucleation of Solid Polar Stratospheric Cloud Particles. *J. Phys. Chem. A* **2002**, *106* (43), 10238–10246.

(4) Tabazadeh, A.; Djikaev, Y. S.; Reiss, H. Surface Crystallization of Supercooled Water in Clouds. *Proc. Natl. Acad. Sci. U.S.A.* **2002**, *99* (25), 15873–15878.

(5) Djikaev, Y. S.; Tabazadeh, A.; Hamill, P.; Reiss, H. Thermodynamic Conditions for the Surface-Stimulated Crystallization of Atmospheric Droplets. *J. Phys. Chem. A* **2002**, *106* (43), 10247–10253.

(6) Kay, J. E.; Tsemekhman, V.; Larson, B.; Baker, M.; Swanson, B. Comment on Evidence for Surface-Initiated Homogeneous Nucleation. *Atmos. Chem. Phys.* **2003**, *3*, 1439–1443.

(7) Turner, G. W.; Bartell, L. S. On the Probability of Nucleation at the Surface of Freezing Drops. *J. Phys. Chem. A* **2005**, *109* (31), 6877–6879.

(8) Koop, T. Homogeneous Ice Nucleation in Water and Aqueous Solutions. *Z. Phys. Chem.* **2004**, *218* (11), 1231–1258.

(9) Duft, D.; Leisner, T. Laboratory Evidence for Volume-Dominated Nucleation of Ice in Supercooled Water Microdroplets. *Atmos. Chem. Phys.* **2004**, *4*, 1997–2000.

(10) Sigurbjornsson, O. F.; Signorell, R. Volume versus Surface Nucleation in Freezing Aerosols. *Phys. Rev. E* **2008**, *77* (5), 051601.

(11) Shaw, R. A.; Durant, A. J.; Mi, Y. Heterogeneous Surface Crystallization Observed in Undercooled Water. *J. Phys. Chem. B* **2005**, *109* (20), 9865–9868.

(12) Durant, A. J.; Shaw, R. A. Evaporation Freezing by Contact Nucleation Inside-Out. *Geophys. Res. Lett.* **2005**, *32* (20), L20814.

(13) Bauerecker, S.; Ulbig, P.; Buch, V.; Vrbka, L.; Jungwirth, P. Monitoring Ice Nucleation in Pure and Salty Water via High-Speed Imaging and Computer Simulations. *J. Phys. Chem. C* **2008**, *112* (20), 7631–7636.

(14) Vrbka, L.; Jungwirth, P. Homogeneous Freezing of Water Starts in the Subsurface. *J. Phys. Chem. B* **2006**, *110* (37), 18126–18129.

(15) Zasetsky, A. Y.; Remorov, R.; Svishchev, I. M. Evidence of Enhanced Local Order and Clustering in Supercooled Water near Liquid−Vapor Interface: Molecular Dynamic Simulations. *Chem. Phys. Lett.* **2007**, *435* (1−3), 50–53.

(16) Hindmarsh, J. P.; Russell, A. B.; Chen, X. D. Observation of the Surface and Volume Nucleation Phenomena in Undercooled Sucrose Solution Droplets. *J. Phys. Chem. C* **2007**, *111* (16), 5977–5981.

(17) Orr, C.; Hurd, F. K.; Hendrix, W. P.; Junge, C. The Behavior of Condensation Nuclei under Changing Humidities. *J. Meteorol.* **1958**, *15* (2), 240–242.

(18) Cohen, M. D.; Flagan, R. C.; Seinfeld, J. H. Studies of Concentrated Electrolyte Solutions Using the Electrodynamic Balance. 3. Solute Nucleation. *J. Phys. Chem.* **1987**, *91* (17), 4583–4590.

(19) Tang, I. N.; Munkelwitz, H. R. Water Activities, Densities, and Refractive Indices of Aqueous Sulfates and Sodium Nitrate Droplets of Atmospheric Importance. *J. Geophys. Res., [Atmos.]* **1994**, *99* (D9), 18801–18808.

(20) Xu, J.; Imre, D.; McGraw, R.; Tang, I. Ammonium Sulfate: Equilibrium and Metastability Phase Diagrams from 40 to−50 °C. *J. Phys. Chem. B* **1998**, *102* (38), 7462–7469.

(21) Han, J. H.; Martin, S. T. Heterogeneous Nucleation of the Efflorescence of $(NH_4)_2SO_4$ Particles Internally Mixed with Al_2O_3, TiO_2, and ZrO_2. *J. Geophys. Res., [Atmos.]* **1999**, *104* (D3), 3543–3553.

(22) Onasch, T. B.; Siefert, R. L.; Brooks, S. D.; Prenni, A. J.; Murray, B.; Wilson, M. A.; Tolbert, M. A. Infrared Spectroscopic Study of the Deliquescence and Efflorescence of Ammonium Sulfate Aerosol as a Function of Temperature. *J. Geophys. Res., [Atmos.]* **1999**, *104* (D17), 21317–21326.

(23) Badger, C. L.; George, I.; Griffiths, P. T.; Braban, C. F.; Cox, R. A.; Abbatt, J. P. D. Phase Transitions and Hygroscopic Growth of Aerosol Particles Containing Humic Acid and Mixtures of Humic Acid and Ammonium Sulphate. *Atmos. Chem. Phys.* **2006**, *6*, 755–768.

(24) Gao, Y. G.; Chen, S. B.; Yu, L. E. Efflorescence Relative Humidity for Ammonium Sulfate Particles. *J. Phys. Chem. A* **2006**, *110* (24), 7602–7608.

(25) Pant, A.; Parsons, M. T.; Bertram, A. K. Crystallization of Aqueous Ammonium Sulfate Particles Internally Mixed with Soot and Kaolinite: Crystallization Relative Humidities and Nucleation Rates. *J. Phys. Chem. A* **2006**, *110* (28), 8701–8709.

(26) Parsons, M. T.; Riffell, J. L.; Bertram, A. K. Crystallization of Aqueous Inorganic−Malonic Acid Particles: Nucleation Rates, Dependence on Size, and Dependence on the Ammonium-to-Sulfate Ratio. *J. Phys. Chem. A* **2006**, *110*, 8108–8115.

(27) Sjogren, S.; Gysel, M.; Weingartner, E.; Baltensperger, U.; Cubison, M. J.; Coe, H.; Zardini, A. A.; Marcolli, C.; Krieger, U. K.; Peter, T. Hygroscopic Growth and Water Uptake Kinetics of Two-Phase Aerosol Particles Consisting of Ammonium Sulfate, Adipic and Humic Acid Mixtures. *J. Aerosol Sci.* **2007**, *38* (2), 157–171.

(28) Middlebrook, A. M.; Murphy, D. M.; Thomson, D. S. Observations of Organic Material in Individual Marine Particles at Cape Grim during the First Aerosol Characterization Experiment (ACE 1). *J. Geophys. Res., [Atmos.]* **1998**, *103* (D13), 16475–16483.

(29) Murphy, D. M.; Cziczo, D. J.; Froyd, K. D.; Hudson, P. K.; Matthew, B. M.; Middlebrook, A. M.; Peltier, R. E.; Sullivan, A.; Thomson, D. S.; Weber, R. J. Single-Particle Mass Spectrometry of Tropospheric Aerosol Particles. *J. Geophys. Res., [Atmos.]* **2006**, *111* (D23), D23S32.

(30) Choi, M. Y.; Chan, C. K. The Effects of Organic Species on the Hygroscopic Behaviors of Inorganic Aerosols. *Environ. Sci. Technol.* **2002**, *36* (11), 2422–2428.

(31) Brooks, S. D.; Garland, R. M.; Wise, M. E.; Prenni, A. J.; Cushing, M.; Hewitt, E.; Tolbert, M. A. Phase Changes in Internally Mixed Maleic Acid/Ammonium Sulfate Aerosols. *J. Geophys. Res., [Atmos.]* **2003**, *108* (D15), 4487.

(32) Pant, A.; Fok, A.; Parsons, M. T.; Mak, J.; Bertram, A. K. Deliquescence and Crystallization of Ammonium Sulfate−Glutaric Acid and Sodium Chloride−Glutaric Acid Particles. *Geophys. Res. Lett.* **2004**, *31* (12), L12111.

(33) Pant, A.; Knopf, D. A.; Bertram, A. K. Deliquescence and Crystallization of Ammonium Sulfate Particles Internally Mixed with Water-Soluble Organic Compounds. *J. Phys. Chem. A* **2004**, *108*, 11600–11608.

(34) Braban, C. F.; Abbatt, J. P. D. A Study of the Phase Transition Behavior of Internally Mixed Ammonium Sulfate−Malonic Acid Aerosols. *Atmos. Chem. Phys.* **2004**, *4*, 1451–1459.

(35) Zardini, A. A.; Sjogren, S.; Marcolli, C.; Krieger, U. K.; Gysel, M.; Weingartner, E.; Baltensperger, U.; Peter, T. A Combined Particle Trap/HTDMA Hygroscopicity Study of Mixed Inorganic/Organic Aerosol Particles. *Atmos. Chem. Phys.* **2008**, *8* (18), 5589–5601.

(36) Marcolli, C.; Krieger, U. K. Phase Changes during Hygroscopic Cycles of Mixed Organic/Inorganic Model Systems of Tropospheric Aerosols. *J. Phys. Chem. A* **2006**, *110* (5), 1881–1893.

(37) Ciobanu, V. G.; Marcolli, C.; Krieger, U. K.; Weers, U.; Peter, T. Liquid−Liquid Phase Separation in Mixed Organic/Inorganic Aerosol Particles. *J. Phys. Chem. A* **2009**, *113* (41), 10966–10978.

(38) Zuend, A.; Marcolli, C.; Luo, B. P.; Peter, T. A Thermodynamic Model of Mixed Organic−Inorganic Aerosols To Predict Activity Coefficients. *Atmos. Chem. Phys.* **2008**, *8* (16), 4559–4593.

(39) Zuend, A.; Marcolli, C.; Peter, T.; Seinfeld, J. H. Computation of Liquid−Liquid Equilibria and Phase Stabilities: Implications for RH-Dependent Gas/Particle Partitioning of Organic−Inorganic Aerosols. *Atmos. Chem. Phys. Discuss.* **2010**, *10*, 12497–12561.

(40) Marcolli, C.; Ciobanu, V. G.; Krieger, U. K.; Zuend, A.; Peter, T. Reversible Phase State Changes at One-Liquid-Phase/Two-Liquid-Phases Boundary. Manuscript in preparation.

(41) Liu, X. Y. Interfacial Effect of Molecules on Nucleation Kinetics. *J. Phys. Chem. B* **2001**, *105*, 11550–11558.

(42) Chan, M. N.; Lee, A. K. Y.; Chan, C. K. Responses of Ammonium Sulfate Particles Coated with Glutaric Acid to Cyclic Changes in Relative Humidity: Hygroscopicity and Raman Characterization. *Environ. Sci. Technol.* **2006**, *40* (22), 6983–6989.

(43) Jackson, K. A. *Kinetic Processes: Crystal Growth, Diffusion and Phase Transition in Materials*; John Wiley & Sons: New York, 2004.

(44) Vergara, A.; Paduano, L.; D'Errico, G.; Sartorio, R. Network Formation in Polyethyleneglycol Solutions. An Intradiffusion Study. *Phys. Chem. Chem. Phys.* **1999**, *1* (20), 4875–4879.

(45) Jones, A. G. *Crystallization Process Systems*; Elsevier Science: New York, 2002.

(46) Wolf, E. *Progress in Optics*, 1st ed.; Elsevier Science: New York, 2000; Vol. 41.

(47) Weis, D. D.; Ewing, G. E. Water Content and Morphology of Sodium Chloride Aerosol Particles. *J. Geophys. Res., [Atmos.]* **1999**, *104* (D17), 21275–21285.

(48) Colberg, C. A.; Krieger, U. K.; Peter, T. Morphological Investigations of Single Levitated $H_2SO_4/NH_3/H_2O$ Aerosol Particles during Deliquescence/Efflorescence Experiments. *J. Phys. Chem. A* **2004**, *108* (14), 2700–2709.

(49) Rasband, W. S. *ImageJ*; U.S. National Institutes of Health: Bethesda, MD, 1997−2009; http://rsb.info.nih.gov/ij/.

(50) Abramoff, M. D.; Magelhaes, P. J.; Ram, S. J. Image Processing with ImageJ. *Biophotonics Int.* **2004**, *11* (7), 36–42.

(51) Cheng, J. A.; Blanchard, D. C.; Cipriano, R. J. The Formation of Hollow Sea-Salt Particles from the Evaporation of Drops of Seawater. *Atmos. Res.* **1988**, *22*, 15–25.

(52) Braun, C.; Krieger, U. K. Two Dimensional Angular Light Scattering in Aqueous NaCl Single Aerosol Particles during Deliquescence and Efflorescence. *Opt. Express* **2001**, *8* (6), 314–321.

(53) Sear, R. P. Nucleation at Contact Lines Where Fluid−Fluid Interfaces Meet Solid Surfaces. *J. Phys.: Condens. Matter* **2007**, *19*, 466106.

(54) Wacaser, B. A.; Dick, K. A.; Johansson, J.; Borgstrom, M. T.; Deppert, K.; Samuelson, L. Preferential Interface Nucleation: An Expansion of the VLS Growth Mechanism for Nanowires. *Adv. Mater.* **2009**, *21* (2), 153–165.

(55) Suzuki, S.; Nakajima, A.; Yoshida, N.; Sakai, M.; Hashimoto, A.; Kameshima, Y.; Okada, K. Freezing of Water Droplets on Silicon Surfaces Coated with Various Silanes. *Chem. Phys. Lett.* **2007**, *445* (1−3), 37–41.

(56) Shahidzadeh-Bonn, N.; Rafai, S.; Bonn, D.; Wegdam, G. Salt Crystallization during Evaporation: Impact of Interfacial Properties. *Langmuir* **2008**, *24* (16), 8599–8605.

(57) Wang, F.; Zhao, L. J.; Zhang, Y. H. Crystallization Dynamics of Supersaturated $NaClO_4$ Aerosols Studied by High-Speed Photography. *Chin. Sci. Bull.* **2008**, *53* (14), 2139–2144.

(58) Deegan, R. D.; Bakajin, O.; Dupont, T. F.; Huber, G.; Nagel, S. R.; Witten, T. A. Contact Line Deposits in an Evaporating Drop. *Phys. Rev. E* **2000**, *62* (1), 756–765.

(59) Henderson, J. A.; Richards, R. W.; Penfold, J.; Thomas, R. K.; Lu, J. R. Organization of Poly(ethylene oxide) Monolayers at the Air−Water Interface. *Macromolecules* **1993**, *26*, 4591–4600.

JP103541W